

This is an Open Access document downloaded from ORCA, Cardiff University's institutional repository: <https://orca.cardiff.ac.uk/id/eprint/140375/>

This is the author's version of a work that was submitted to / accepted for publication.

Citation for final published version:

Thomas, Sophie R. and Casini, Angela 2021. N-Heterocyclic carbenes as “smart” gold nanoparticle stabilizers: state-of-the art and perspectives for biomedical applications. *Journal of Organometallic Chemistry* 938 , 121743. 10.1016/j.jorganchem.2021.121743

Publishers page: <http://dx.doi.org/10.1016/j.jorganchem.2021.121743>

Please note:

Changes made as a result of publishing processes such as copy-editing, formatting and page numbers may not be reflected in this version. For the definitive version of this publication, please refer to the published source. You are advised to consult the publisher's version if you wish to cite this paper.

This version is being made available in accordance with publisher policies. See <http://orca.cf.ac.uk/policies.html> for usage policies. Copyright and moral rights for publications made available in ORCA are retained by the copyright holders.



N-Heterocyclic carbenes as “smart” gold nanoparticle stabilizers: State-of-the art and perspectives for biomedical applications

Sophie R. Thomas ^{a,b}, Angela Casini ^{b,*}

^a School of Chemistry, Cardiff University, Main Building, Park Place, CF10 3AT Cardiff, United Kingdom

^b Medicinal and Bioinorganic Chemistry, Department of Chemistry, Technical University of Munich, Lichtenbergstr. 4, 85747 Garching, Germany

article info

Keywords:

N-heterocyclic carbenes
Gold nanoparticles
Gold complexes
Organometallics
Nanomaterials
Biomedicine

abstract

The unique properties and high synthetic flexibility of N-heterocyclic carbenes (NHCs) have made them highly attractive tools for the development of new nanomaterials and the fundamental study of their properties. In this review, we focus on the case of NHC-stabilized gold nanoparticles (NHC@AuNPs) with potential for biological applications. AuNPs are ubiquitous in biomedicine, where they serve as versatile scaffolds for drug/gene delivery, biosensing, imaging and therapy. In this context, our review aims at presenting an overview of the relatively few studies reporting on the synthesis and characterization of NHC@AuNPs, with emphasis on the strategies adopted to achieve water-soluble biocompatible nanoparticles. Overall, the possible combinatorial design of NHC ligand shell functionality opens to new perspectives for this relatively unexplored research area.

1. Introduction

Gold nanoparticles (AuNPs) have attracted much attention over the last few decades in the fields of materials, [1,2] catalysis [3] and medicine, [4–6] also due to their optical properties, [7,8] biocompatibility and well-established synthetic protocols to control their size and morphology. [9] In such nano-assemblies, the size of the aggregates and interparticle distances within the structure govern the final collective properties of the resulting materials. For biomedical applications, these variations in morphology, size, and functionality are directly correlated to the AuNPs biodistribution, biological half-life, renal secretion, cellular internalization, and plasmon optical properties. [10–13] Because of the latter, gold nanoparticles are inherently *theranostic*, providing imaging contrast through near infrared (NIR) fluorescence, X-ray, [14,15] photoacoustic, [16,17] and Raman enhancement, [18] and act as a vehicle to enhance ablative therapies both for photothermal and X-ray radiation. [19–23] In recent years, AuNPs have also been used as nanocarriers for transition metal catalysts for bio-orthogonal transformations in cells. [24]

One major challenge in the field of nanomaterial design is to achieve sufficient metal nanoparticle stability for the desired application. In fact, ‘stability’ is a broad concept, describing the preser-

vation of a particular nanostructure property, ranging from aggregation, composition, crystallinity, shape, size, and surface chemistry. [25] In practice, the definition of nanoparticle stability depends on the targeted size-dependent property that is pursued and can only exist for a finite period of time given all nanostructures are inherently thermodynamically and energetically unfavorable relative to the respective bulk states. Over the years, in order to enhance the AuNPs’ stability and to tune their surface properties, a number of capping ligands have been developed, through which colloidal stabilization originates from a combination of electrostatic repulsion and steric isolation. Several amongst such capping agents feature sulfur containing groups with high binding affinity to ‘soft’ Au surfaces. Thus, a variety of ligands have been employed to functionalize metallic gold, particularly sulfur-based compounds like thiols, sulfides or disulfides, with high packing density. [26] In 1994, Brust et al. [27] reported the first example of thiol stabilized AuNPs using the alkanethiol dodecanethiol, ranging between 1 and 3 nm in size, which remained a popular synthetic choice over the years. Later on, in a seminal paper, Rotello and coworkers developed water soluble amphiphilic AuNPs capped with octanethiol/11-thioundecanoic acid, whose assembly was controlled by pH. [28]

Despite the numerous examples, the S–Au bond is not strong enough to confer long-term stability to the derived materials. Therefore, N-heterocyclic carbenes (NHCs) have emerged as surface ligands for metal NPs due to their ability to form strong covalent bonds to metallic surfaces. [29] Another advantage of using NHCs

* Corresponding author.

E-mail address: angela.casini@tum.de (A. Casini).

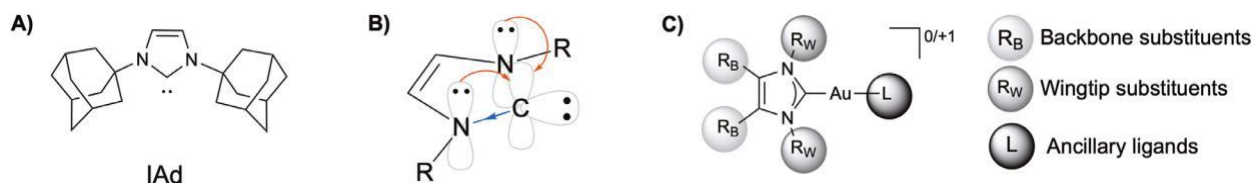


Fig. 1. (A) Structure of **IAd** (1,3-bis(adamantyl)imidazol-2-ylidene); (B) Representation of singlet ground state electronic structure of imidazol-2-ylidene-type NHC; (C) General structure of Au(I) NHC complexes and possible modifications.

as ligands is the possibility of modification of the N-heterocyclic scaffold with different functional groups affording a tunable surface, as it will be discussed in the next sections.

2. Properties of N-heterocyclic carbene ligands

Following the isolation of the stable carbene (1,3-bis(adamantyl)imidazol-2-ylidene) (**IAd**, Fig. 1A) in 1991, [30] N-heterocyclic carbenes have gained significant attention due to their great stability and ease of derivatization, allowing a broad library of NHCs to be produced within a relatively short period of time. [31–33] The σ -electron-withdrawing and π -electron-donating nitrogen atoms next to the carbene carbon stabilize the NHC by lowering the energy of the occupied σ -orbital and increasing the electron density in the empty p orbital. Furthermore, the cyclic NHC structure confers additional stabilization to the singlet sp^2 hybridized carbene state (Fig. 1B). The formally divalent carbon species features several advantages, such as straightforward synthesis and robustness towards functionalization enabling structural diversity and catalytic activity. [31,32,34] Currently, NHCs are privileged ligands for a wide range of main group, transition metal, and f-block species, [35,36] being highly modular in nature leading to their large structural and stereoelectronic diversity. NHCs are prepared most commonly from (benz)imidazolylidenes, as well as from pyrazolylidene, triazolylidene, tetrazolylidene, thiazolylidenes, oxazolylidenes and oxadiazolylidenes scaffolds or from their so-called ‘abnormal’ zwitterionic counterparts. The majority of NHCs feature a five-membered ring scaffold, although a number of ‘ring-expanded’ analogues based on tetrahydropyrimidine, triazine, diazepane and diazocane rings have also been reported. [31] Furthermore, cyclic (alkyl)(amino)carbenes (CAACs) were discovered in 2005 by Bertrand and coworkers, [37] featuring different electronic properties due to the substitution of one of the π -electron donating amino groups with a σ -donating alkyl group. This results in CAACs being more nucleophilic (σ -electron donating) and more electrophilic (π -electron accepting) than ‘classical’ NHCs. [38]

The neutral, electron-rich NHCs form a strong covalent bond with metallic surfaces, which is the key to the stabilization of metal NPs, enabling them to maintain their size-dependent properties. [39] Although NHC-stabilized mono/oligo-atomic elemental species have been synthesized and characterized as early as 1994,

[40] the first evidence for NHC–metal NP interactions appeared in 2005 and 2007. [41,42] Since then a range of different NHC-functionalized metal NPs (NHC@MNPs) have been synthesized.

To fine-tune the strength of the metal coordination environment and therefore, the stability of the NHC-metal fragment, derivatization of the backbone scaffold has important influence, as well as modifications of the wingtip position (Fig. 1C). The latter can sterically affect the carbene-metal bond favoring stability of the resulting metal complexes, as well as preventing aggregation in the case of NHC@MNPs. [39] Moreover, wingtip-derivatization can increase water solubility [43] or be exploited to generate surface-bound initiators for catalytic applications. [44] The broad structural variety of NHCs contrasts with thiol ligands, whose interfa-

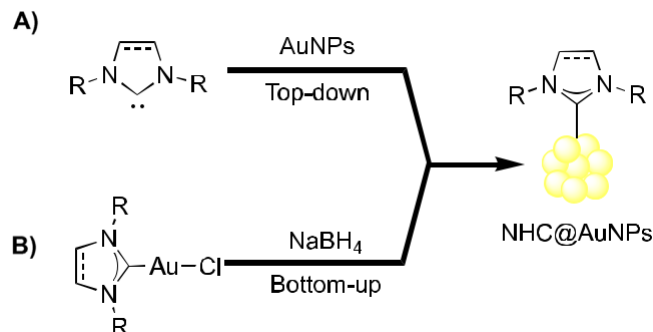


Fig. 2. General schemes of the (A) top-down synthesis and (B) bottom-up synthesis of NHC@AuNPs.

cial properties are mainly determined by the head group of the alkyl chain as a consequence of the close packing at the NPs surface. [26] Despite these advantages, to date, the number of examples of NHC-stabilized metal (Au) NPs is still limited and numerous applications remain unexplored, particularly in the areas of biomedicine, photoacoustic (PA) imaging, photothermal therapy (PTT) and biosensing. The reader is referred to more comprehensive reviews for an overview of the field. [29,39,45]

3. NHC stabilized gold nanoparticles

Two main approaches have been applied for the synthesis of gold NPs stabilized by NHC ligands (NHC@AuNPs): *i*) the ‘top-down’ and *ii*) the ‘bottom-up’ approach, respectively (Fig. 2).

[45] In 2009, Chechik and coworkers [46] were the first to prepare NHC-functionalized AuNPs *via* ligand exchange of didodecyl sulfide (DDS)-protected AuNPs (‘top-down’ synthesis, Fig. 2A). These NPs remained unchanged in size after ligand exchange as determined by transmission electron microscopy (TEM). X-ray photo-electron spectroscopy (XPS) revealed an absence of thioether ligands and the appearance of a single peak at 400.3 eV in the N 1s region, which was assigned to the surface-bound NHC. [46] However, the NPs formed insoluble precipitates in solution after some hours, and mono- and bis-NHC Au complexes were observed as degradation products. On the basis of these results, it was hypothesized that the mechanism of AuNP instability involved desorption of these complexes from the surface leading to NP aggregation. [46] Shortly afterwards, Tilley and Vignolle [47] applied for the first time the ‘bottom-up’ synthesis of redispersible NHC-stabilized AuNPs with long alkyl chains as wingtip groups, by reduction of Au(I) NHC complexes (Fig. 2B). This method produced

monocrystalline 5–7 nm AuNPs which were stable in organic solvents for months. This study also reported on the influence of the type of reducing agent on the size and shape of the resulting AuNPs. [47] Since then, AuNPs with various NHC ligands synthesized following one of the two main approaches have been reported.

In a somehow related ‘bottom-up’ approach, involving reduction of an Au(I) NHC precursor, Richeter and coworkers [48] developed a method for synthesizing ultra-small AuNPs coated with

NHCs *via* thermolysis of preformed or *in situ* generated heteroleptic Au(I) NHC complexes bearing pentafluorophenyl as ancillary ligand, under solvent-free conditions. The AuNPs were found to be smaller than 2 nm and were applied as catalysts, loaded onto aminopropyl-functionalized silica support, in the reduction of 4-nitrophenol. [48] Such ultra-small AuNPs could be suitable for in-tracellular drug delivery due to their increased stability in the presence of serum components, [49] or as a near-infrared imaging agent for *in vivo* fluorescence detection of tumor cells. [50] Another useful method to achieve NHC@AuNPs applied deprotonation of imidazolium haloaurate salts followed by their *in situ* reduction; [51,52] however, spectroscopic characterization of the resulting particles suggested the presence of some unidentified NHC-derived impurities.

The effect of different NHC ligands for NP formation was investigated using 1,3-diethylbenzimidazol-2-ylidene, 1,3-bis(mesityl)imidazol-2-ylidene, and 1,3-bis(2,6-*i*Pr₂C₆H₃)imidazol-2-ylidene carbene scaffolds. [53] The latter scaffold, characterized by increased steric bulk, produced AuNPs of smaller average size (2.7 nm) and larger size distribution (12.5%) with respect to the other two NHCs (producing nanoparticles of 6.5 – 6.6 nm and narrow size distributions of 6.7% and 4.6%, respectively). Overall, the efficiency of the process and the average size and size distribution of the nanoparticles markedly depended on the nature of the NHC ligand, on the sequence of reactant addition (*i.e.*, presence or absence of thiol during the reduction step), and on the presence of oxygen. [53]

Four small (<1.6 nm diameter) calix[4]arene NHC-bound gold clusters were synthesized following the bottom-up method.

[54] The smallest calix[4]arene NHC-bound Au cluster consisted of a 1.2 nm gold core, and its number density of accessible and open surface sites was measured using a SAMSA (5-((2-(and-3)-S-(acetylmercapto)succinoyl)amino)) fluorescein dye molecule. The number density of open Au sites on the new calix[4]arene NHC-bound AuNPs measured by the SAMSA fluorescein probe strongly supports the generality of a mechanical model of accessibility, which does not depend on the functional group involved in binding to the gold surface and rather depends on the relative radii of curvature of bound ligands and the gold cluster core. [54]

Conductive polymer-AuNP hybrids were also synthesized by disproportionation of Au(I) to Au(III) and Au(0), with concomitant reduction of Au(III) by oxidatively coupling bithiophenes linked to the NHC ligands in the starting Au(I) complexes. [55] TEM images of the synthesized NHC-CP/AuNP hybrids indicated that spherical AuNPs of average size *ca.* 3.6 nm were well-dispersed with narrow size distributions. Since the isolated NHC-CP/AuNPs were not soluble in organic solvents, their analysis was performed by ¹³C solid-state NMR spectroscopy, showing a signal in the region appropriate for a carbene C–Au bond (185.5 ppm), supporting the idea that NHC groups help the dispersion of AuNPs in the polymer matrix. The NHC@AuNPs were also active towards the reduction of 4-nitrophenol. [55]

In 2014, Glorius, Ravoo, and coworkers [56] demonstrated that the introduction of long alkyl chains at C4 and C5 of the imidazolylidene ligand, and use of small or flexible N-substituents, enabled the preparation of “air”-stable and aggregation-stable NHC@AuNPs. These NPs were formed following the top-down strategy, *via* ligand exchange on thioether-stabilized AuNPs. The effects of the type of NHC ligand on the AuNPs formation were further studied by Richeter and coworkers, [57] who reported on the reaction of thioether-stabilized gold nanoparticles generated *in situ* with benzimidazol-2-ylidene ligands. In this case, the NHC@AuNPs were two times smaller than the thioether-stabilized NPs precursors,

with a mean size of 2.8 (±0.6) nm, and more aggregated, as shown by TEM and by the broad SPR observed at $\lambda_{\text{max}} \sim 552$ nm.

[57] Such an evolution of the AuNP morphology suggests that lig-

and exchange is not the only process occurring at the AuNPs surface, and that the reaction with NHCs also leads to etching. Interestingly, using several characterization techniques in the solid state, including ¹³C solid state NMR and powder X-ray diffraction (XRD), it was possible to demonstrate that (i) the formation of bis-carbene Au(I) complexes occurs in concomitance to NHC@AuNPs formation, and that (ii) residual NHC ligands are present at the AuNPs surface. [57] One possible interpretation of the quantitative formation of the bis-carbene Au(I) complex would be that the initially generated NHC-Au containing species are weakly bound to the NP surface, and may be released to further react with the remaining NHC generated *in situ*. This process occurs also in the case of *in situ* generated imidazol-2-ylidenes. Interestingly, the bis-NHC Au(I) complexes may be interacting with the AuNP surface by aurophilic interactions, as discussed in another study. [58] In the latter, starting from citrate capped AuNPs, the synthesis of NHC@AuNPs was achieved using dinuclear Au(I)-bridged flexible macrocycles whereby the gold centers were bound by the NHC scaffold. [58] Unfortunately, the binding of the NHCs to the NP surface could not be undoubtedly characterized.

A few years later, the binding modes of NHCs on the gold surface were studied in depth by a combination of scanning tunneling microscopy, XPS, and density functional theory (DFT) calculations.

[59] In detail, the impact of alkyl side groups on the formation of NHC species at the Au(111) surface was elucidated, whereby two significantly different binding modes depending on the alkyl chain length were identified. Whilst longer alkyl groups resulted exclusively in NHC-Au-NHC complexes lying flat on the surface, stabilized by van der Waals interactions, the short alkyl substituents favored an up-standing NHC configuration with one Au atom extracted from the surface. [59]

In 2018, Crudden and coworkers [60] reported on AuNPs stabilized by bidentate N-heterocyclic carbene (NHC) ligands, synthesized by either top-down or bottom-up approaches. The selected NHCs featured a benzimidazole scaffold with the backbone appended by alkyl groups and a connecting alkyl chain bridging the NHC moieties *via* the wingtip positions (Fig. 3A). As a general trend, smaller nanoparticles resulted from the bottom-up reductive approach compared with the top-down ligand exchange method (Fig. 3B). The presence of the NHC on the AuNPs surface was confirmed by XPS and thermogravimetric analysis (TGA). [60] Whilst the appearance of the N (1 s) signal at 401 eV typical of the presence of NHCs on surfaces was detected, higher ligand desorption temperatures were also observed for NHC-stabilized AuNPs (obtained by the top-down approach) compared to thiol functionalized ones, as well as for alkylated or bidentate NHCs vs non-alkylated or monodentate NHCs, respectively. AuNPs prepared by the bottom-up method showed greater propensity to ripen upon heating, likely to be due to the smaller initial size of the NPs, or lower ligand density. [60] Finally, the stability of the NHC@AuNPs was tested towards thiols, such as DTT and thiophenol, by UV-Visible spectroscopy. Of note, while the top-down synthesized NPs with bidentate NHCs featured remarkable stability, the corresponding bottom-up NPs showed initial changes upon thiol treatment and more significant decomposition after 48 h. [60]

The versatility of NHC@AuNPs was next showcased by Cao et al. in 2016, [61] where the efficient electrocatalytic reduction of CO₂ to CO in water was reported. The nanoparticles were formed by the top-down approach, whereby oleylamine stabilized AuNPs were added to an excess of the ligand in anhydrous toluene, resulting in ligand exchange.

In an attempt to obtain water-soluble AuNPs *via* the bottom-up method, NHCs tethered to *N*-BOC-histidine-methyl ester group (BOC = *tert*-butoxycarbonyl) *via* the heterocyclic backbone were synthesized. [62] Thus, chiral histidine-derived Au(I) NHC complexes, chlorido-(1,3-dimethyl-*N*-BOC-O-methyl-*L*/*D*-histidin-2-

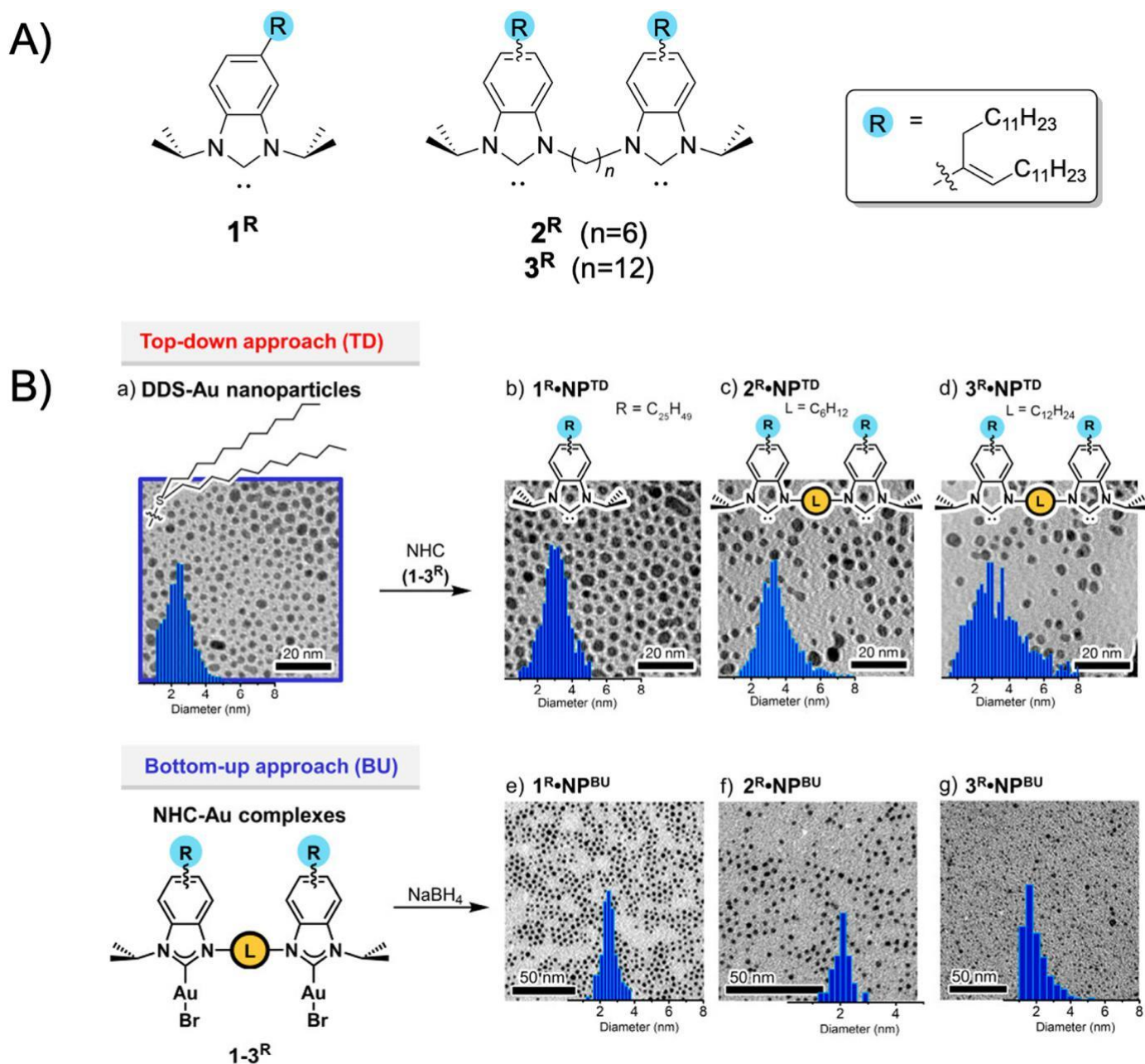


Fig. 3. (A) Structure of the bidentate NHC ligands used of the synthesis of NHC@AuNPs *via* top-down and bottom-up approaches. [60] (B) TEM images and particle size distributions of AuNPs stabilized by DDS (dodecyl sulfide) or NHCs. Reproduced with permission from ref. [60] Copyright (2018) American Chemical Society.

ylidene)Au(I), were reduced by ^tBuNH₂·BH₃ (*tert*-Butylamine bo-rane) in THF to afford AuNPs showing a bimodal size distribution. Nanoparticle size selection was carried out by centrifugation of the AuNP suspensions, enabling isolation of monodisperse nanoparticles. Circular dichroism (CD) spectroscopy showed optical activity of the AuNPs arising from the chiral NHC ligands, but not for the Au(I) NHC complexes, indicating that packing of the NHCs on the nanoparticle surface is crucial to enable chiral activity. [62] Unfortunately, *N*-BOC deprotection did not afford water soluble AuNPs, but produced aggregates which were not soluble in a variety of protic and aprotic solvents.

An alternative application of chiral NHC ligands for AuNP synthesis was later published by Toste and coworkers, [63] based on the concept of supported Dendrimer-Encapsulated Metal Clusters (DEMCs). The AuNPs were formed by reduction of the chiral Au(I) NHC complex with ^tBuNH₂·BH₃, in the presence of the

dendrimer. The resulting dendrimer-encapsulated AuNPs were then added to the silica support, followed by separation from the solution to prevent NP aggregation. XPS studies reflected the prevalence of Au(I) species at the surface of NHC@AuNPs, also confirmed by high-resolution mass spectrometry. [63] To further understand how far beyond the NPs surface the oxidation state differences persisted, a bulk analysis technique, namely X-ray absorption near edge structure (XANES), was applied. The obtained results indicated that over 95% of Au atoms were in the Au(0) phase. The NHC-ligated AuNP catalysts enabled a model lactonization reaction to proceed at 20 °C, while NHC-free AuNPs are inactive below 80 °C. [63] Of note, the NHC-capping of the AuNPs led to asymmetric induction (up to 16% enantiomeric excess) in the lactonization transformations. Varying the chiral NHC ligands enabled initial structure-activity relationships to be inferred, including: *i*) steric bulk of the NHC wingtip groups did not correlate with cat-

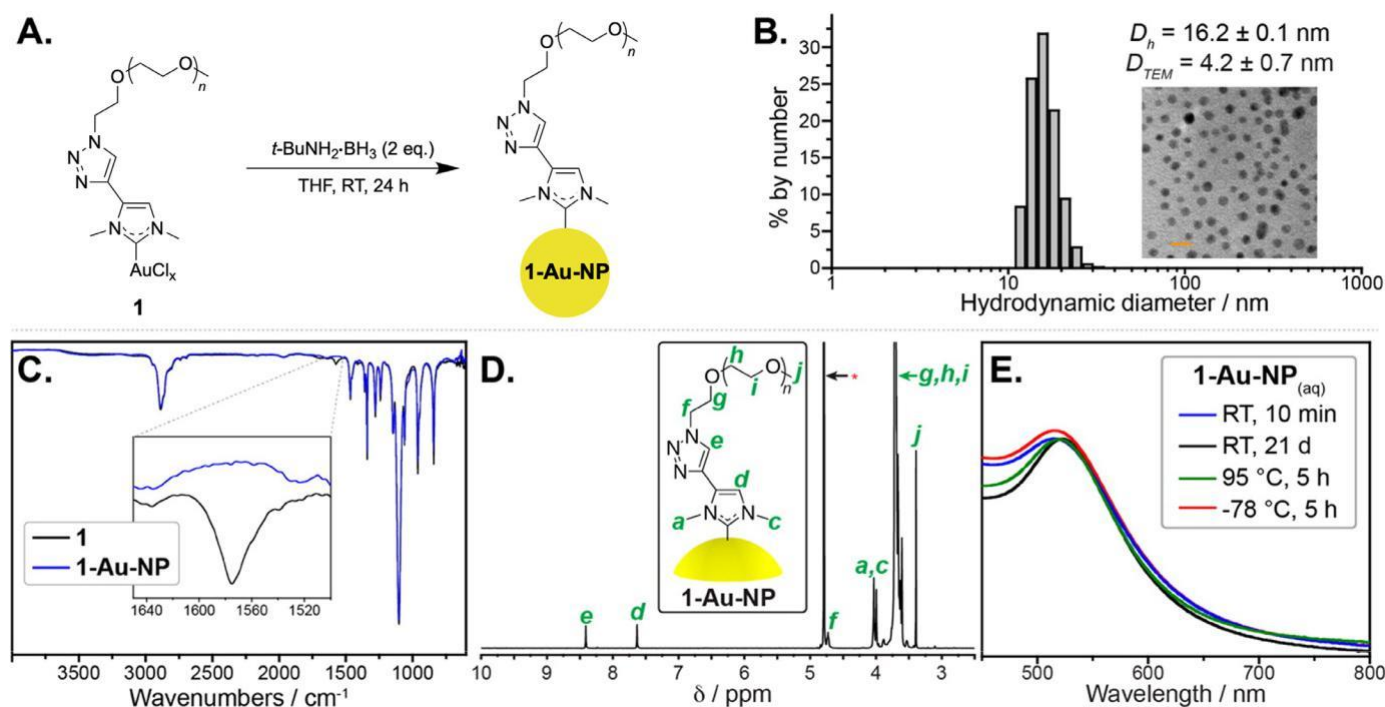


Fig. 4. Water-soluble PEGylated NHC@AuNPs. (A) Synthetic scheme of Au(I) NHC complex reduction to form AuNP (1-Au-NP). (B) Dynamic light scattering (DLS) histogram for aqueous solution of PEGylated NHC@AuNP; inset: TEM image of these AuNPs. (C) ATR-FTIR spectra for starting imidazolium salt and PEGylated NHC@Au NP; inset: peak corresponding to coordination of Au to the imidazolium salt. (D) ^1H NMR spectrum of PEGylated NHC@AuNP. “*” = residual solvent peak. (E) UV-Vis spectra showing the surface plasmon band (SPB) for PEGylated NHC@AuNP(aq) after exposure to various conditions. Adapted with permission from ref. [65] Copyright (2015) American Chemical Society.

alyst’s activity, *ii*) more likely, increased NHC ligand rigidity in the same order led to a less dense Au NHC complex packing on the NP surface, thereby enabling reactant access to the active sites, and *iii*) the presence of hydroxyl groups on one of the wingtips sub-stituents was critical to enable catalyst activity, most likely facilitating the turnover-limiting proto-deauration through H-bonding interactions. [63] Overall, this study shows that attachment of NHC on the surface of AuNPs not only activates the catalysts, but also installs a handle to control enantioselectivity.

3.1. Water-soluble NHC-stabilized AuNPs: synthesis and biological applications

The water-stability (solubility) of gold NPs is an important pre-requisite for their biomedical applications, and is a great challenge in nanotechnology. It should be noted that the first example of water-soluble metal NPs stabilized by NHC ligands was published by the groups of Chaudret and de Jesús in 2014, [64] reporting on highly stable NHC@PtNPs that could be formed using hydrophilic sulfonated NHC ligands *via* a bottom-up approach. Subsequently, following the same method, the first example of water-soluble NHC@AuNPs was reported by MacLeod and Johnson in 2015. [65] PEGylated AuNPs were formed by reduction of the corresponding Au(I)/Au(III) NHC complexes with $t\text{BuNH}_2\text{BH}_3$ in THF at room temperature (Fig. 4, Table 1), followed by dialysis against water. A mixture of Au(I) and Au(III) NHC complexes were used as precursors due to separation issues. TEM and dynamic light scattering measurements confirmed the presence of a polymeric shell around the gold core (Fig. 4B). The attenuated total reflectance Fourier transform infrared (ATR-FTIR) spectra of the related imidazolium salt and NHC@AuNPs were very similar, confirming the presence of the PEGylated ligand onto the NP surface. However, the lack of the imidazolium key vibrational band (at $\sim 1576\text{ cm}^{-1}$) in the nanoparticle specimen (Fig. 4C) strongly suggested that the

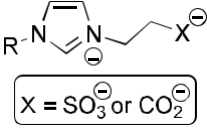
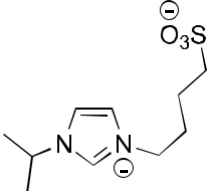
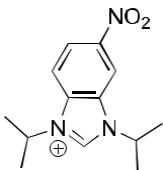
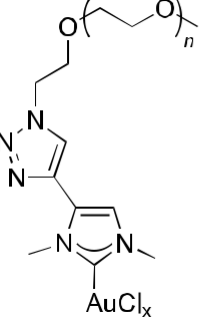
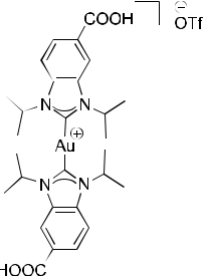
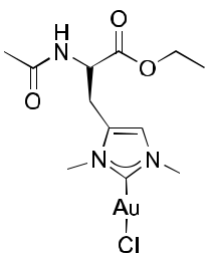
NHC is coordinated to the Au surface. UV-Vis spectroscopy of these PEGylated NHC@AuNPs revealed that they were stable for at least 3 months in aqueous solution, as well as in NaCl solutions below 250 mM for 6 h. Aqueous NP solutions above pH 3 were also very stable, *i.e.* after 8 weeks the SPR band decreased only slightly, with a small red shift. The NPs also showed durability against extreme temperatures (95 and -78°C) for 5 h (Fig. 4E), and remained dispersed and stable in cell culture media containing fetal bovine serum (FBS) for 26 h at 37°C , as evidenced by the unaffected surface plasmon band (SPB). [65] The effect of thiols on the PEGylated NHC@AuNPs was monitored by UV-Vis spectroscopy and ^1H NMR, and different rates of reactivity and induced aggregation were observed. [65]

In 2017, Crudden and coworkers [66] reported on the synthesis of an amphiphilic NHC-Au(I) complex based on an asymmetric triethylene glycol-/dodecyl-functionalized benzimidazole, which was further used to prepare the corresponding stable amphiphilic NHC-decorated AuNPs, whose self-assembly behavior was studied in polar solvents (water and EtOH). [66] While relatively small islands of NHC@AuNP ensembles were observed for the sample in water, higher order aggregation was evident for nanoparticles self-assembled in EtOH. It should be noted that it is the aggregation numbers of the AuNPs clusters as well as the interparticle distances within the structures that change in this process, not the discrete AuNPs size. In fact, the average diameter of the AuNPs within the aggregates formed in water and EtOH, was found to be 4.1 ± 1.3 nm and 4.3 ± 1.3 nm after 24 h, respectively. [66] Unfortunately, due to the formation of NP aggregates, these systems are not suitable for biological applications.

The same group presented water-soluble NHC@AuNPs formed by a ‘bottom-up’ approach. In detail, the $[\text{Au}(\text{NHC})\text{Cl}]$ complex and corresponding bis-NHC complex $[(\text{NHC})_2\text{Au}]\text{OTf}$ (NHC = carboxylated benzimidazolylidene, Fig. 5A, Table 1) were reduced using sodium borohydride (NaBH_4) in an aqueous solution of sodium hy-

Table 1

Examples of water-soluble AuNPs stabilized by NHC ligands, including method of synthesis, size, stability in biologically relevant conditions and explored application.

NHC Ligand	Details	Size (nm)	Stability	Application	Reference
Top-down approach					
	<ul style="list-style-type: none"> Starting material DDS (didodecylsulfide) capped AuNPs. - NHC deprotonated <i>in situ</i> with KO^tBu in biphasic hexane/DMF system. 	4.1 – 4.9	All NPs stable at pH >4 for months in aqueous solution.	Not tested	Ravoo and Glorius, 2015 [68]
	<ul style="list-style-type: none"> Starting material OAm (oleyamine) capped Au_xPd_y NPs NHC deprotonated <i>in situ</i> with KO^tBu in DMF. 	4.0	N/A	Aerobic oxidation of d-glucose (aqueous solution), and semihydrogenation of diphenylacetylene by transfer hydrogenation and hydrogenation of nitroarenes (solid support)	Ravoo and Glorius, 2018 [69]
	<ul style="list-style-type: none"> Starting material citrate capped AuNPs in DCM/H₂O mixture. No external reductant required. 	ca. 18	N/A	Not tested	Jenkins and Camden, 2020 [70]
Bottom-up approach					
	<ul style="list-style-type: none"> Au(I)/Au(III) NHC complex pre-synthesized before reduction with <i>t</i>-BuNH₂ BH₃ in THF, for 24 h. 	4.2 ± 0.7	Stable in pH range of 3–14 over 2 months, and in various biologically relevant conditions. Moderate stability towards GSH over 26 h.	Not tested	Johnson, 2015 [65]
	<ul style="list-style-type: none"> Au(I) NHC complex pre-synthesized before reduction with NaBH₄ in water, for 5 h. 	2.4 ± 0.3	Moderate stability in 150 mM NaCl solution after 7d, and after exposure to 2 mM GSH over 24 h.	Probe for photoacoustic imaging	Nambo and Crudden, 2017 [67]
	<ul style="list-style-type: none"> (i) Au(I) NHC complex pre-synthesized before reduction with <i>t</i>-BuNH₂ BH₃ in THF, 16 h. (ii) Hydrolysis of ethyl ester group with NaOH in H₂O/EtOH for 1 h at 90 °C. 	4.2 ± 1.2	Moderate stability in aqueous solutions (pH 3–13), stable up to 36 days in PBS (pH 7.4) and NaCl solution (150 mM), and stable for 48 h in GSH (2 mM, pH 8)	Not tested	Chin and Reithofer, 2019 [71]

(continued on next page)

Table 1 (continued)

NHC Ligand	Details	Size (nm)	Stability	Application	Reference
	Reduction of $\text{HAuCl}_4 \cdot 3\text{H}_2\text{O}$ with NaBH_4 in water in the presence of the imidazolium salt.	5.6 ± 1.5	N/A	Catalyzed the A^3 coupling of aldehydes, terminal alkynes and amines in neat conditions to afford propargylamines, and the cycloisomerization of γ -alkynoic acids to enol lactones in toluene: H_2O (1:1)	Pleixats, 2020 [72]
Top-down and adatom approach					
	(i) Ligand exchange with CTAB coated Au nanorods. (ii) Reduction of AuNHC with $t\text{-BuNH}_2 \cdot \text{BH}_3$ in THF, 24 h.	Length: 42.6 ± 6.7 Width: 9.9 ± 1.3	Nanorods stable over a range of different pHs and temperatures, as well as with excess GSH and in cell culture media.	Use in PTT. Preliminary tests successful in MCF7 cancer cells <i>in vitro</i> .	Johnson, 2019 [73]

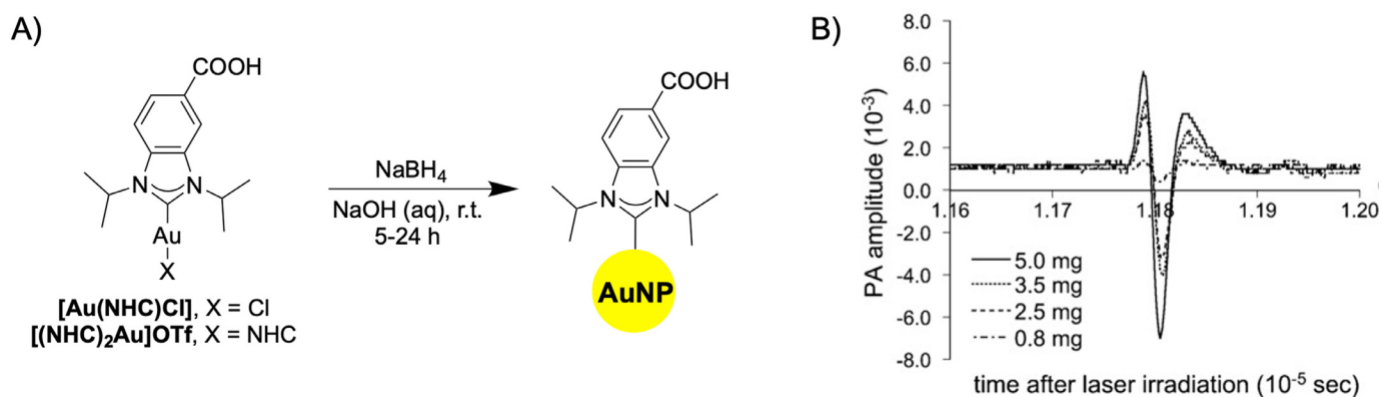


Fig. 5. (A) Structures of mono- and bis-NHC Au(I) complexes used for the formation of water soluble AuNPs; (B) Acoustic wave signal recorded after irradiation of an aqueous solution of NHC@AuNPs (different concentrations) at 532 nm using a pulsed laser beam. Image adapted with permission from ref. [67] Copyright (2017) John Wiley and Sons.

dioxide (NaOH). [67] NaOH is required to deprotonate the carboxylate group on the NHC ligand, forming water soluble AuNPs with a negatively charged surface. The size of the nanoparticles (between 2 and 4 nm) and the intensity of the SPR band could be controlled by varying the reaction time. [67] Interestingly, the evolution of the NHC-Au nanoparticles to larger sizes proceeded homogeneously, affording NHC@AuNPs with narrow size distributions after 7 and 24 h, as evaluated by TEM and gel electrophoresis. Next, the stability of the NPs was assessed in basic solutions at pH 8 and 10 for 2 months, showing very little change in UV-Vis spectra over time. [67] To better mimic biological media, the stability of the NHC@AuNPs was assessed in 150 mM NaCl solution, and showed high stability with only a slight sharpening of the SPR band after 7 days. The larger NPs were also moderately stable in excess GSH under slightly basic conditions (pH 8) over 24 h. For the first time, the NHC@AuNPs were tested for biomedical applications as possible probes for photoacoustic imaging. [67] Thus, an aqueous solution of AuNPs was prepared and irradiated with a pulsed laser beam (532 nm). Despite their weak SPR bands, the sample gave a reliable photoacoustic signal, which increased linearly with the NHC@AuNPs concentration (Fig. 5B). [67]

In 2019, the groups of Chin and Reithofer [71] achieved water-soluble NHC@AuNPs by the bottom up approach (Table 1) using NHC ligands derived from a *N*-acetyl-L-histidine ethyl ester scaffold

and featuring either a methyl or isopropyl group on the wingtips of the imidazole ring. The Au(I) NHC complexes were subsequently reduced to AuNPs using $t\text{-BuNH}_2 \cdot \text{BH}_3$ in THF at room temperature for 16 h. [71] To obtain water soluble AuNPs, they were then saponified with NaOH in an EtOH/ H_2O mixture for 1 h at 90 °C. TEM analysis confirmed the presence of AuNPs with a size range of ca. 4 nm. The NHC@AuNPs bearing methyl groups as wingtips showed much higher stability compared to the isopropyl derivatives across a range of different conditions, including phosphate buffer solution (PBS, pH 7.4), aqueous NaCl solution (150 mM) and in the presence of glutathione (GSH, 2 mM, pH 8). [71] The stability of the NPs in the presence of GSH was also investigated by ^1H NMR; in this case no change was observed over 24 h suggesting that the thiol group of GSH is unable to displace the NHC ligand on the AuNPs. The steric bulk of the isopropyl group was proposed to be the cause of reduced stability compared to the AuNPs with the methyl wingtips, [71] in line with previous studies on a family of sterically demanding NHC ligands. [56] UV-Vis spectroscopy also showed the pH dependent reversible aggregation of the NHC@AuNPs, due to protonation of the carboxylic acid moiety. [71]

Recently, the use of PEGylated imidazolium (bromide and tetrafluoroborate) and tris-imidazolium (bromide) salts containing triazole linkers, as stabilizers for the preparation of water-

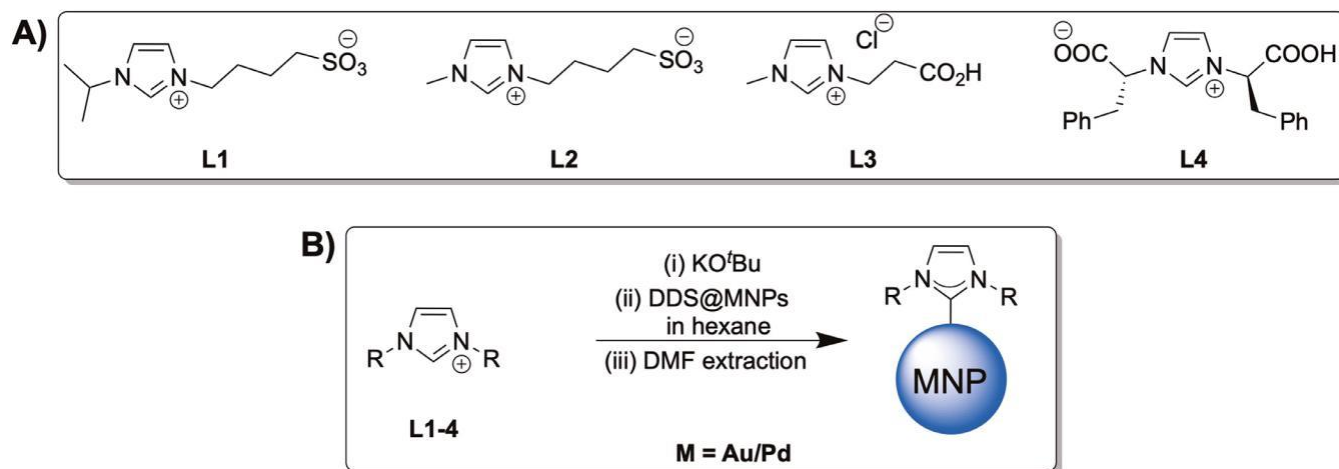


Fig. 6. (A) Structures of imidazolium salts **L1-L4** used as stabilizers for water soluble MNPs ($M = \text{Au}$ and Pd); (B) Reaction scheme to form NHC@MNPs from **L1-4**. [68].

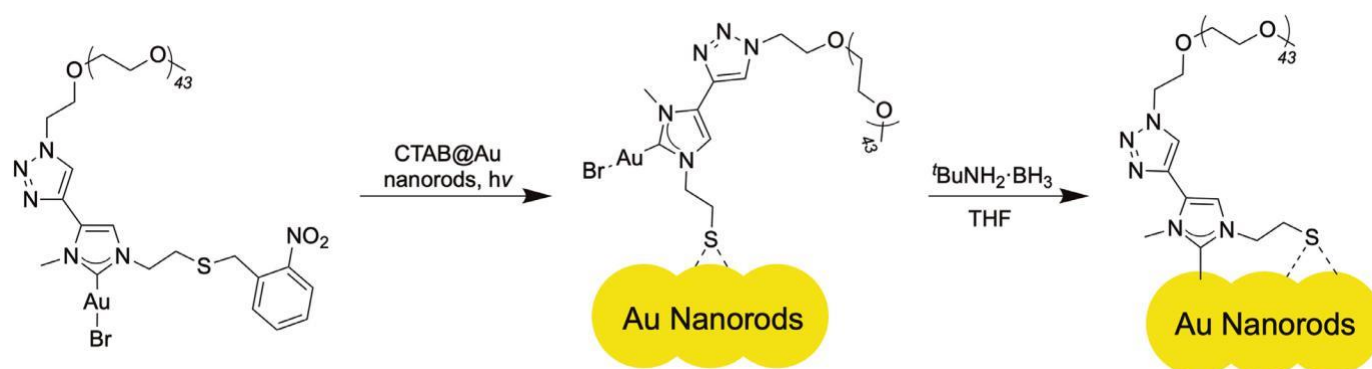
soluble gold nanoparticles by reduction of tetrachloroauric acid (HAuCl_4) with NaBH_4 was reported (Table 1). [72] TEM analysis confirmed the formation of spherical and well-dispersed nanoparticles of mean diameters from 4.5 to 5.6 nm. Unfortunately, whilst a number of spectroscopic data indicate that the heterocycle ligand is close to the surface of the metal, no conclusive experimental evidence with respect to its nature, either imidazolium or carbene, could be obtained. [72] It should be noted that, in general, although NHCs have been demonstrated as suitable ligands for the stabilization of gold nanoparticles through a variety of methods, the mechanism by which such NHC@AuNPs form is yet to be fully elucidated. For example, XPS studies of chiral (L/D)-histidin-2-ylidene stabilized gold nanoparticles, formed using well defined organometallic Au(I) complexes, showed the concomitant presence of Au(I) and Au(0) in the nanoparticles. [74] Based on this observation, it was postulated that AuNPs synthesized from Au(I) NHC complexes exhibit a monolayer of Au(I) surrounding a Au(0) core, but further studies are necessary to elucidate this hypothesis.

In 2015, following the top-down approach, water soluble PdNPs and AuNPs, stabilized by negatively charged NHC ligands bearing either sulfonate or carboxylate groups as wingtip substituents, were reported. [68] The NPs were formed using the didodecylsulfide (DDS)-stabilised Pd or AuNPs as precursors in a biphasic mixture of hexane and DMF (dimethylformamide). In detail, the reactive NHCs were formed *in situ* in DMF from their corresponding imidazolium salts by addition of KO^tBu , before addition of DDS-metal NPs (Fig. 6, Table 1). Of note, the NHC AuNPs showed a significant decrease in size upon ligand exchange, with DDS@AuNPs having a mean size of 8.5 ± 1.7 nm, whereas NHC@AuNPs featured a mean size of 4.7 ± 1.6 nm. [68] From pH 4 and below, the carboxylated AuNPs formed aggregates, most likely due to the protonation of the carboxylic function, while the sulfonate AuNPs were stable. When kept under basic conditions, the NPs could repeatedly be dried and redispersed in aqueous media without size alterations. [68]

Following the top-down approach, recent work by Camden, Jenkins and coworkers [70] reported a general method for synthesising NHC@AuNPs with protic groups, formed in aqueous conditions with an average diameter >15 nm (Table 1). In contrast to thiols, functionalizing NHCs with protic groups is challenging; however, such groups are essential as they are routinely applied in sensing, [75] biological applications, [76] as a precursor to amide couplings [77,78] and widely exploited for bioconjugation reactions of metal NHCs to biomolecules. [79] In detail, addition of bis- and mono-NHC Au(I) complexes to citrate-capped AuNPs led

to replacement of the citrate group with the NHC ligand on the NPs in water (with an organic co-solvent). [70] Using this robust and reproducible approach, nitro-functionalized AuNPs were used as intermediates and reduced *in situ* to form amine-functionalized NHC nanoparticles. The amine NHCs could easily undergo amide coupling with a model carboxylic acid and L-phenylalanine, opening up the large space of applications afforded by the amide-linkage. [70] Of note, the relatively large size of the aforementioned NHC@AuNPs is ideal for selected biological applications, requiring NPs greater than 10 nm to avoid rapid exclusion by the kidneys, [80] and for detection by surface-enhanced Raman scattering (SERS), which is most efficient with NPs between 20 and 100 nm. [81]

To broaden the scope of NHC@AuNPs, the synthesis of non-spherical NPs was reported by Johnson and coworkers, [73] who used a bidentate thiolate-NHC-Au(I) complex grafted onto commercial cetyltrimethylammonium bromide (CTAB)-stabilized gold nanorods through ligand exchange. First, exchange of CTAB ligands on commercial CTAB@Au nanorods with a photogenerated thiolate was achieved, followed by NHC installation (Fig. 7, Table 1). Upon mild reduction (with 2 equiv. $t\text{BuNH}_2\text{-BH}_3$ in THF) of the resulting surface-tethered Au(I) NHC complexes, the gold atom attached to the NHC complex is added to the surface as an adatom (Fig. 7). [73] The concept of bidentate NHCs on nanoparticles was first described by Ravoo, Glorius and coworkers [82] using similar bidentate hybrid NHC-thioether ligands to stabilize PdNPs, which remained spherical and small in size and were successful catalysts for the chemoselective hydrogenation of olefins. [82] This strategy avoids the need for reorganization of the underlying surface lattice upon NHC binding. Such an elegant approach was inspired by the often observed etching of gold surfaces by free NHCs, [46,57,83] and by previous data showing that when NHCs are deposited onto planar gold substrates under ultrahigh vacuum, they tend to abstract a gold atom from the surface lattice to generate translationally mobile NHC@Au adatom complexes. [84] The resulting thiolate-NHC-stabilized gold nanorods were water soluble thanks to the functionalization of the NHC backbone with triazole-conjugated polyethylene glycol. The nanoparticles were also stable towards excess glutathione for up to six days, and under conditions with large variations in pH (from 2 to 14), low and high temperatures (between -78°C to 95°C), high salt concentrations (up to 1 M NaCl), or in biological and cell culture media. Of note, in this work the obtained NHC@AuNPs were applied for PTT *in vitro*, showing selective cancer cell-killing only upon laser irradiation. [73]



Recent work by Ravoo, Glorius and coworkers [69] described, for the first time, bimetallic NPs stabilized by NHC ligands, combining the advantageous properties of both Au and Pd nanoparticles. The water soluble NPs (ca. 4 nm average diameter) were formed by the ‘top-down approach’ involving the ligand exchange of oleylamine (OAm)-stabilized Au_xPd_y with the *in situ* generated NHC ligand (Table 1). [69] The $\text{NHC}@_{\text{Au}_x\text{Pd}_y}\text{NPs}$ were explored as biomimetic catalysts for the aerobic oxidation of D-glucose, which is catalyzed naturally by glucose oxidase, and showed considerable catalytic activity. [69] Considering that the NP performance increases with higher Au content, gold was supposed to be the actual active metal, while the alloy effect confers superior colloidal stability with respect to the monometallic $\text{NHC}@_{\text{AuNPs}}$ analogues. The $\text{Au}_x\text{Pd}_y\text{NPs}$ were also supported on TiO_2 , and, as such, successfully catalyzed the semihydrogenation of diphenylacetylene, showing switchable selectivity towards the (Z)- or (E)-stilbene product, and the hydrogenation of nitroarenes. [69]

- [12] X.D. Zhang, D. Wu, X. Shen, P.X. Liu, F.Y. Fan, S.J. Fan, *Biomaterials* 33 (2012) 4628–4638.
- [13] B.D. Chithrani, A.A. Ghazani, W.C.W. Chan, *Nano Lett.* 6 (2006) 662–668.
- [14] R. Chehelatani, R.M. Ezzibdeh, P. Chhour, K. Pulaparthi, J. Kim, M. Jurcova, J.C. Hsu, C. Blundell, H.I. Litt, V.A. Ferrari, H.R. Alcock, C.M. Sehgal, D.P. Cormode, *Biomaterials* 102 (2016) 87–97.
- [15] P. Chhour, J. Kim, B. Benardo, A. Tovar, S. Mian, H.I. Litt, V.A. Ferrari, D.P. Cormode, *Bioconjug. Chem.* 28 (2017) 260–269.
- [16] D. Pan, M. Pramanik, A. Senpan, J.S. Allen, H. Zhang, S.A. Wickline, L.V. Wang, G.M. Lanza, *FASEB J.* 25 (2011) 875–882.
- [17] D. Pan, M. Pramanik, A. Senpan, S. Ghosh, S.A. Wickline, L.V. Wang, G.M. Lanza, *Biomaterials* 31 (2010) 4088–4093.
- [18] H. Jang, K. Kang, M.A. El-Sayed, *J. Mater. Chem. B* 6 (2018) 5460–5465.
- [19] X. Wang, S. Gao, Z. Qin, R. Tian, G. Wang, X. Zhang, L. Zhu, X. Chen, *ACS Appl. Mater. Interfaces* 10 (2018) 15140–15149.
- [20] Y. Ma, X. Liang, S. Tong, G. Bao, Q. Ren, Z. Dai, *Adv. Funct. Mater.* 23 (2013) 815–822.
- [21] X.Y. Su, P.D. Liu, H. Wu, N. Gu, *Cancer Biol. Med.* 11 (2014) 86–91.
- [22] R.S. Norman, J.W. Stone, A. Gole, C.J. Murphy, T.L. Sabo-Attwood, *Nano Lett.* 8 (2008) 302–306.
- [23] W. Yang, H. Liang, S. Ma, D. Wang, J. Huang, *Sustain. Mater. Technol.* 22 (2019) 1–12.
- [24] G.Y. Tonga, Y. Jeong, B. Duncan, T. Mizuhara, R. Mout, R. Das, S.T. Kim, Y.C. Yeh, B. Yan, S. Hou, V.M. Rotello, *Nat. Chem.* 7 (2015) 597–603.
- [25] H.T. Phan, A.J. Haes, *J. Phys. Chem. C* 123 (2019) 16495–16507.
- [26] S. Engel, E.C. Fritz, B.J. Ravoo, *Chem. Soc. Rev.* 46 (2017) 2057–2075.
- [27] M. Brust, M. Walker, D. Bethell, D.J. Schiffrin, R. Whyman, *J. Chem. Soc., Chem. Commun.* (1994) 801–802.
- [28] J. Simard, C. Briggs, A.K. Boal, V.M. Rotello, *Chem. Commun.* (2000) 1943–1944.
- [29] C.A. Smith, M.R. Narouz, P.A. Lumis, I. Singh, A. Nazemi, C.-H. Li, C.M. Cruden, *Chem. Rev.* 119 (2019) 4986–5056.
- [30] A.J. Arduengo, R.L. Harlow, M. Kline, *J. Am. Chem. Soc.* 113 (1991) 361–363.
- [31] M.N. Hopkinson, C. Richter, M. Schedler, F. Glorius, *Nature* 510 (2014) 485–496.
- [32] D.J. Nelson, S.P. Nolan, *Chem. Soc. Rev.* 42 (2013) 6723–6753.
- [33] S. Díez-González, N. Marion, S.P. Nolan, *Chem. Rev.* 109 (2009) 3612–3676.
- [34] M.J. Schultz, M.S. Sigman, *N-Heterocycl. Carbenes Synth.* (2006) 103–118.
- [35] T. Scatollin, S.P. Nolan, *Trends Chem.* 2 (2020) 721–736.
- [36] A. Doddi, M. Peters, M. Tamm, *Chem. Rev.* 119 (2019) 6994–7112.
- [37] V. Lavallo, Y. Canac, C. Präsang, B. Donnadiou, G. Bertrand, *Angew. Chem. Int. Ed.* 44 (2005) 5705–5709.
- [38] M. Soleilhavoup, G. Bertrand, *Acc. Chem. Res.* 48 (2015) 256–266.
- [39] A.V. Zhukhovitskiy, M.J. MacLeod, J.A. Johnson, *Chem. Rev.* 115 (2015) 11503–11532.
- [40] A.J. Arduengo, S.F. Gamper, J.C. Calabrese, F. Davidson, *J. Am. Chem. Soc.* 116 (1994) 4391–4394.
- [41] L.S. Ott, S. Campbell, K.R. Seddon, R.G. Finte, *Inorg. Chem.* 46 (2007) 10335–10344.
- [42] L.S. Ott, M.L. Cline, M. Deetlefs, K.R. Seddon, R.G. Finte, *J. Am. Chem. Soc.* 127 (2005) 5758–5759.
- [43] L.A. Schaper, S.J. Hock, W.A. Herrmann, F.E. Kühn, *Angew. Chem. Int. Ed.* 52 (2013) 270–289.
- [44] A.V. Zhukhovitskiy, M.G. Mavros, T. Van Voorhis, J.A. Johnson, *J. Am. Chem. Soc.* 135 (2013) 7418–7421.
- [45] Y.Y. An, J.G. Yu, Y.F. Han, *Chin. J. Chem.* 37 (2019) 76–87.
- [46] E.C. Hurst, K. Wilson, I.J.S. Fairlamb, V. Chechik, *New J. Chem.* 33 (2009) 1837–1840.
- [47] J. Vignolle, T.D. Tilley, *Chem. Commun.* (2009) 7230–7232.
- [48] J. Crespo, Y. Guari, A. Ibarra, J. Larionova, T. Lasanta, D. Laurencin, J.M. López-De-Luzuriaga, M. Monge, M.E. Olmos, S. Richeter, *Dalt. Trans.* 43 (2014) 15713–15718.
- [49] A.A. Sousa, J.T. Morgan, P.H. Brown, A. Adams, M.P.S. Jayasekara, G. Zhang, C.J. Ackerson, M.J. Kruhlak, R.D. Leapman, *Small* 8 (2012) 2277–2286.
- [50] X. Wu, X. He, K. Wang, C. Xie, B. Zhou, Z. Qing, *Nanoscale* 2 (2010) 2244–2249.
- [51] C.J. Serpell, J. Cookson, A.L. Thompson, C.M. Brown, P.D. Beer, *Dalt. Trans.* 42 (2013) 1385–1393.
- [52] X. Ling, S. Roland, M.P. Pileni, *Chem. Mater.* 27 (2015) 414–423.
- [53] X. Ling, N. Schaeffer, S. Roland, M.P. Pileni, *Langmuir* 29 (2013) 12647–12656.
- [54] M.M. Nigra, A.J. Yeh, A. Okrut, A.G. Dipasquale, S.W. Yeh, A. Soloviyov, A. Katz, *Dalt. Trans.* 42 (2013) 12762–12771.
- [55] S.G. Song, C. Satheeshkumar, J. Park, J. Ahn, T. Premkumar, Y. Lee, C. Song, *Macromolecules* 47 (2014) 6566–6571.
- [56] C. Richter, K. Schaepe, F. Glorius, B.J. Ravoo, *Chem. Commun.* 50 (2014) 3204–3207.
- [57] M. Rodríguez-Castillo, D. Laurencin, F. Tielens, A. Van Der Lee, S. Clément, Y. Guari, S. Richeter, *J. Chem. Soc. Dalt. Trans.* 43 (2014) 5978–5982.
- [58] H.X. Liu, X. He, L. Zhao, *Chem. Commun.* 50 (2014) 971–974.
- [59] A. Bakker, A. Timmer, E. Kolodzeiski, M. Freitag, H.Y. Gao, H. Mönig, S. Amirjalayer, F. Glorius, H. Fuchs, *J. Am. Chem. Soc.* 140 (2018) 11889–11892.
- [60] R.W.Y. Man, C.-H. Li, M.W.A. MacLean, O.V. Zenkina, M.T. Zamora, L.N. Saunders, A. Rousina-Webb, M. Nambo, C.M. Crudden, *J. Am. Chem. Soc.* 140 (2018) 1576–1579.
- [61] Z. Cao, D. Kim, D. Hong, Y. Yu, J. Xu, S. Lin, X. Wen, E.M. Nichols, K. Jeong, J.A. Reimer, P. Yang, C.J. Chang, *J. Am. Chem. Soc.* 138 (2016) 8120–8125.
- [62] A.J. Young, C.J. Serpell, J.M. Chin, M.R. Reithofer, *Chem. Commun.* 53 (2017) 12426–12429.
- [63] R. Ye, A.V. Zhukhovitskiy, R.V. Kazantsev, S.C. Fakra, B.B. Wickemeyer, F.D. Toste, G.A. Somorjai, *J. Am. Chem. Soc.* 140 (2018) 4144–4149.
- [64] E.A. Baquero, S. Tricard, J.C. Flores, E. De Jesus, B. Chaudret, *Angew. Chem. Int. Ed.* 53 (2014) 13220–13224.
- [65] M.J. MacLeod, J.A. Johnson, *J. Am. Chem. Soc.* 137 (2015) 7974–7977.
- [66] M.R. Narouz, C.H. Li, A. Nazemi, C.M. Crudden, *Langmuir* 33 (2017) 14211–14219.
- [67] K. Salorinne, R.W.Y. Man, C.H. Li, M. Taki, M. Nambo, C.M. Crudden, *Angew. Chem. Int. Ed.* 56 (2017) 6198–6202.
- [68] A. Ferry, K. Schaepe, P. Tegeder, C. Richter, K.M. Chepiga, B.J. Ravoo, F. Glorius, *ACS Catal.* 5 (2015) 5414–5420.
- [69] P. Tegeder, M. Freitag, K.M. Chepiga, S. Muratsugu, N. Möller, S. Lamping, M. Tada, F. Glorius, B.J. Ravoo, *Chem. Eur. J.* 24 (2018) 18682–18688.
- [70] J.F. DeJesus, L.M. Sherman, D.J. Yohannan, J.C. Becca, S.L. Strausser, L.F.P. Karger, L. Jensen, D.M. Jenkins, J.P. Camden, *Angew. Chem. Int. Ed.* 59 (2020) 7585–7590.
- [71] A.J. Young, C. Eisen, G.M.D.M. Rubio, J.M. Chin, M.R. Reithofer, *J. Inorg. Biochem.* 199 (2019) 1–9.
- [72] G. Fernández, L. Bernardo, A. Villanueva, R. Pleixats, *New J. Chem.* 44 (2020) 6130–6141.
- [73] M.J. MacLeod, A.J. Goodman, H.Z. Ye, H.V.T. Nguyen, T. Van Voorhis, J.A. Johnson, *Nat. Chem.* 11 (2019) 57–63.
- [74] A.J. Young, M. Sauer, G.M.D.M. Rubio, A. Sato, A. Foelske, C.J. Serpell, J.M. Chin, M.R. Reithofer, *Nanoscale* 11 (2019) 8327–8333.
- [75] B. Sharma, P. Bugga, L.R. Madison, A.I. Henry, M.G. Blaber, N.G. Greeneltch, N. Chiang, M. Mrksich, G.C. Schatz, R.P. Van Duyne, *J. Am. Chem. Soc.* 138 (2016) 13952–13959.
- [76] X. Li, S.M. Robinson, A. Gupta, K. Saha, Z. Jiang, D.F. Moyano, A. Sahar, M.A. Rile, V.M. Rotello, *ACS Nano* 8 (2014) 10682–10686.
- [77] T. Zhang, P. Chen, Y. Sun, Y. Xing, Y. Yang, Y. Dong, L. Xu, Z. Yang, D. Liu, *Chem. Commun.* 47 (2011) 5774–5776.
- [78] C.M. Alexander, K.L. Hamner, M.M. Maye, J.C. Dabrowiak, *Bioconjug. Chem.* 25 (2014) 1261–1271.
- [79] S.M. Meier-Menches, A. Casini, A. Casini, *Bioconjug. Chem.* 31 (2020) 1279–1288.
- [80] N. Hoshyar, S. Gray, H. Han, G. Bao, *Nanomedicine* 11 (2016) 673–692.
- [81] N.D. Israelsen, C. Hanson, E. Vargis, *Sci. World J.* (2015) 1–12.
- [82] A. Rühling, K. Schaepe, L. Rakers, B. Vönhören, P. Tegeder, B.J. Ravoo, F. Glorius, *Angew. Chem. Int. Ed.* 55 (2016) 5856–5860.
- [83] C.M. Crudden, J.H. Horton, I.I. Ebralidze, O.V. Zenkina, A.B. McLean, B. Drevniok, Z. She, H.B. Kraatz, N.J. Mosey, T. Seki, E.C. Keske, J.D. Leake, A. Rousina-Webb, G. Wu, *Nat. Chem.* 6 (2014) 409–553.
- [84] G. Wang, A. Rühling, S. Amirjalayer, M. Knor, J.B. Ernst, C. Richter, H.J. Gao, A. Timmer, H.Y. Gao, N.L. Doltsinis, F. Glorius, H. Fuchs, *Nat. Chem.* 9 (2017) 152–156.
- [85] H.H. Chang, M.T. Gole, C.J. Murphy, *MRS Bull.* 45 (2020) 387–393.
- [86] Ö. Karaca, V. Scalcon, S.M. Meier-Menches, R. Bonsignore, J.M.J.L. Brouwer, F. Tonolo, A. Folda, M.P. Rigobello, F.E. Kühn, A. Casini, *Inorg. Chem.* 56 (2017) 14237–14250.
- [87] C.H.G. Jakob, B. Dominelli, E.M. Hahn, T.O. Berghausen, T. Pinheiro, F. Marques, R.M. Reich, J.D.G. Correia, F.E. Kühn, *Chem. Asian J.* 15 (2020) 2754–2762.
- [88] M.A. Reynoso-Esparza, I.I. Rangel-Salas, A.A. Peregrina-Lucano, J.G. Alvarado-Rodríguez, F.A. López-Dellamary-Toral, R. Manríquez-González, M.L. Espinosa-Macías, S.A. Cortes-Llamas, *Polyhedron* 81 (2014) 564–571.
- [89] A. Bakker, M. Freitag, E. Kolodzeiski, P. Bellotti, A. Timmer, J. Ren, B. Schulze Lammers, D. Moock, H.W. Roesky, H. Mönig, S. Amirjalayer, H. Fuchs, F. Glorius, *Angew. Chem. Int. Ed.* 59 (2020) 13643–13646.
- [90] G.M.D.M. Rubio, B.K. Keppler, J.M. Chin, M.R. Reithofer, *Chem. Eur. J.* 26 (2020) 15859–15862.
- [91] A. Villa, N. Dimitratos, C.E. Chan-Thaw, C. Hammond, G.M. Veith, D. Wang, M. Manzoli, L. Prati, G.J. Hutchings, *Chem. Soc. Rev.* 45 (2016) 4953–4994.